Analyst

PAPER

View Article Online
View Journal

Cite this: DOI: 10.1039/c6an00144k

Quantification of tunicamycin-induced protein expression and *N*-glycosylation changes in yeast†

Haopeng Xiao, Johanna M. Smeekens and Ronghu Wu*

Tunicamycin is a potent protein *N*-glycosylation inhibitor that has frequently been used to manipulate protein glycosylation in cells. However, protein expression and glycosylation changes as a result of tunicamycin treatment are still unclear. Using yeast as a model system, we systematically investigated the cellular response to tunicamycin at the proteome and *N*-glycoproteome levels. By utilizing modern mass spectrometry-based proteomics, we quantified 4259 proteins, which nearly covers the entire yeast proteome. After the three-hour tunicamycin treatment, more than 5% of proteins were down-regulated by at least 2 fold, among which proteins related to several glycan metabolism and glycolysis-related pathways were highly enriched. Furthermore, several proteins in the canonical unfolded protein response pathway were up-regulated because the inhibition of protein *N*-glycosylation impacts protein folding and trafficking. We also comprehensively quantified protein glycosylation changes in tunicamycin-treated cells, and more than one third of quantified unique glycopeptides (168 of 465 peptides) were down-regulated. Proteins containing down-regulated glycopeptides were related to glycosylation, glycoprotein metabolic processes, carbohydrate processes, and cell wall organization according to gene ontology clustering. The current results provide the first global view of the cellular response to tunicamycin at the proteome and glycoproteome levels.

Received 22nd January 2016,
Accepted 17th March 2016

DOI: 10.1039/c6an00144k

www.rsc.org/analyst

Introduction

Glycosylation is a prevalent protein modification in eukaryotic cells that plays essential roles in regulating protein folding, trafficking and stability.[1–3] Aberrant glycosylation is frequently related to human disease, including cancer and infectious diseases.[3–11] In eukaryotic cells, *N*-glycosylation typically begins with the synthesis of the dolichol-linked precursor oligosaccharide ($GlcNAc_2Man_9Glc_3$), followed by *en bloc* transfer of the precursor oligosaccharide to newly synthesized peptides in the endoplasmic reticulum (ER).[12,13] Then the oligosaccharide is further trimmed and modified by many enzymes in the Golgi apparatus.[14] The pathway for *N*-glycosylation synthesis is conserved from yeast to mammalian cells.[15] Although yeast primarily contains high-mannose glycans which differ from those in mammalian cells,[16] it can still be used as an excellent model system to study protein *N*-glycosylation.[17]

Tunicamycin (TM), a glucosamine-containing antibiotic, blocks N-linked glycosylation by inhibiting the formation of the *N*-acetylglucosamine-dolichol-phosphate intermediate and thus traps cells in the G1 phase of the cell cycle.[17] TM was originally isolated and utilized for its antiviral activity by suppressing viral glycoprotein synthesis and membrane genesis.[18] Now tunicamycin is extensively used for protein *N*-glycosylation manipulation. In yeast, the presence of TM has been reported to disrupt the formation of the external glycoprotein invertase, acid phosphatase, and cell wall mannan.[19] Although the mechanism responsible for TM-initiated inhibition of protein *N*-glycosylation has long been appreciated, a comprehensive and quantitative analysis of the affected proteome and glycoproteome in cells has yet to be conducted.

In recent years, MS-based proteomics methods have become increasingly powerful to systematically study protein expression and modification changes in complex biological samples.[20–32] However, it is still challenging to investigate low-abundance proteins, which requires effective fractionation or other sample preparation.[33–37] Furthermore, the global analysis of glycoproteins in complex biological samples is extraordinarily difficult because of the high heterogeneity of glycans and low abundance of many glycoproteins.[38] Enrichment of glycopeptides and the generation of a common mass tag on glycosylation sites are required prior to MS analysis. In our recent study, based on a common feature of glycans, *i.e.* multiple hydroxyl groups in each glycan, boronic acid-based

School of Chemistry and Biochemistry and the Petit Institute for Bioengineering and Bioscience, Georgia Institute of Technology, Atlanta, Georgia 30332, USA.
E-mail: ronghu.wu@chemistry.gatech.edu; Fax: +404-894-7452; Tel: +404-385-1515

†Electronic supplementary information (ESI) available: Detailed LC gradients (Table S-1-3) protein quantification, glycosylation site identification, glycopeptide quantification, and glycosylation site quantification results (Table S-4-7); analysis of glycosylation site quantification (Fig. S-1). See DOI: 10.1039/c6an00144k

enrichment was used to effectively enrich glycopeptides in yeast whole cell lysates.[39] By incorporating this enrichment method, it is possible to comprehensively quantify protein glycosylation changes with quantitative proteomics.

Using yeast as a model system, we systematically investigated the cell response to TM at the proteome and *N*-glycoproteome levels. We quantified 4259 proteins, which nearly covers the entire yeast proteome. Many proteins related to several glycan metabolism and glycolysis-related pathways were down-regulated in TM-treated cells. We also globally quantified protein *N*-glycosylation changes as a result of the TM treatment. Among down-regulated glycoproteins, those related to glycosylation, glycoprotein metabolic processes, carbohydrate processes, and cell wall organization were highly enriched. The current results clearly demonstrate that there are dramatic protein expression and *N*-glycosylation changes resulting from the tunicamycin treatment.

Experimental section

Yeast strains, SILAC labeling, and TM treatment conditions

Yeast (*Saccharomyces cerevisiae*) cells were seeded in "heavy" (Lys^8 ($^{13}C_6$ and $^{15}N_2$); Arg^6 ($^{13}C_6$) Cambridge isotopes) or "light" (Lys^0, Arg^0) media (synthetic complete medium with lysine and arginine drop-out) and cultured overnight. Tunicamycin (TM) (Cayman Chemicals) stock solution (10 mg mL^{-1}) was prepared by dissolving TM in dimethyl sulfoxide (DMSO). When the cell population had undergone more than ten doubling times and reached the exponential growth phase (OD = 0.3 at 600 nm), TM (2 μg mL^{-1}) was added into the "heavy" media while the "light" cells were treated by the same amount of DMSO as a vehicle control. After treatment for three hours, cells were harvested and mixed at a 1 : 1 ratio based on measured protein concentrations.

Cell lysis, protein extraction and digestion

Cells were washed twice with deionized water, pelleted by centrifugation at 4000*g* for 5 minutes, and then resuspended in lysis buffer (50 mM 4-(2-hydroxyethyl)-1-piperazineethanesulfonic acid (HEPES) pH = 7.6, 150 mM NaCl, 0.5% sodium deoxycholate (SDC), 20 U mL^{-1} benzonase, and 1 protease inhibitor tablet per 10 mL buffer). Cell lysis was performed using a Mini-Beadbeater (Biospec), three 30 second cycles at maximum speed, with 2 minute pauses on ice in between each cycle. Lysates were then centrifuged at 15 000*g* for 10 minutes and the resulting supernatant was transferred into a new tube. The protein concentration was measured by a bicinchoninic acid (BCA) assay (Pierce) and proteins were subjected to disulfide reduction with 5 mM dithiothreitol (DTT) (56 °C, 25 minutes) and alkylation with 14 mM iodoacetamide (RT, 20 minutes in the dark). Detergents were removed by methanol-chloroform protein precipitation. The purified proteins were digested with 10 ng μL^{-1} Lys-C (Wako) in buffer containing 50 mM HEPES pH = 8.6, 1.6 M urea, and 5% ACN, at 31 °C for 16 hours, followed by further digestion with 8 ng μL^{-1} Trypsin (Promega) at 37 °C for 4 hours.

Peptide separation, fractionation, and glycopeptide enrichment

Protein digestions were acidified by the addition of trifluoroacetic acid (TFA) to a final concentration of 0.1%, followed by centrifugation to remove the precipitate. Then peptides were desalted using a tC18 Sep-Pak cartridge (Waters). Purified peptides were aliquoted into two portions: ~0.5 mg for protein analysis and a ~8 mg for glycosylation analysis. For protein analysis, lyophilized peptides were fractionated into 20 fractions by high pH reversed-phase high-performance liquid chromatography (HPLC) with a 40 minute gradient of 5–55% ACN in 10 mM ammonium acetate (pH = 10), and then desalted again using stage-tips. For glycosylation analysis, the separation and enrichment of glycopeptides was carried out by utilizing the covalent interaction between boronic acid and glycans containing multiple hydroxyl groups, as described previously.[39] Peptides were directly subjected to glycopeptide enrichment without HPLC fractionation (the enriched glycopeptide sample was separated into three fractions during the later stage-tip step). Briefly, the peptide mixture was dissolved in 200 mM ammonium acetate buffer (pH = 10), and incubated with boronic acid-conjugated magnetic beads at 37 °C for 1 h. The beads were then washed five times with the binding buffer to remove non-specifically bound peptides. Glycopeptides were eluted by incubating the beads in a solution containing acetonitrile, water, and trifluoroacetic acid at a respective ratio of 50 : 49 : 1 for 30 minutes at 37 °C. Eluates were desalted using tC18 Sep-Pak cartridges and lyophilized overnight.

PNGase F treatment for glycopeptides

Glycopeptides were deglycosylated with five units of peptide-*N*-glycosidase F (PNGase F, Sigma-Aldrich) in 100 μL buffer containing 50 mM NH_4HCO_3 (pH = 9) in heavy-oxygen water ($H_2{}^{18}O$) for 3 h at 37 °C.[40,41] The reaction was quenched by adding formic acid (FA) to a final concentration of 1%. Peptides were further purified *via* stage-tip and separated into 3 fractions using 20%, 50% and 80% ACN containing 1% HOAc.

LC-MS/MS analysis

All purified and dried peptide fractions were dissolved in a solvent containing 5% ACN and 4% FA, and a fraction of each sample was loaded onto a microcapillary column packed with C18 beads (Magic C18AQ, 3 μm, 200 Å, 100 μm × 16 cm, Michrom Bioresources) by a Dionex WPS-3000TPLRS autosampler (UltiMate 3000 thermostatted Rapid Separation Pulled Loop Wellplate Sampler). For protein analysis, peptides were separated by reversed-phase liquid chromatography using an UltiMate 3000 binary pump with a 90 minute gradient of 4–30% ACN containing 0.125% FA. For the enriched glycopeptide samples, a 110 minute gradient of 3–25%, 8–38%, or 10–50% ACN with 0.125% FA was used for each of the three fractions, and the detailed LC gradients are in Table S-1-3.† Peptides were detected with a data-dependent method[42,43] in a

hybrid dual-cell quadrupole linear ion trap – Orbitrap mass spectrometer (LTQ Orbitrap Elite, ThermoFisher, with Xcalibur 3.0.63 software). For each cycle, one full MS scan (resolution: 60 000) in the Orbitrap (10^6 AGC target) was followed by up to 20 MS/MS in the LTQ for the most intense ions. The selected ions were excluded from further sequencing for 90 seconds. Ions with single or unassigned charges were not selected for MS/MS scans. Maximum ion accumulation times were 1000 ms for each full MS scan and 50 ms for MS/MS scans.

Database search and data filtering

Raw mass spectra were converted into mzXML format, and then searched using the SEQUEST algorithm (version 28).[44] The following parameters were used during the search: 10 ppm precursor mass tolerance; 1.0 Da product ion mass tolerance; fully digested with trypsin; up to three missed cleavages; fixed modifications: carbamidomethylation of cysteine (+57.0214); variable modifications: oxidation of methionine (+15.9949), ^{18}O tag on asparagine (+2.9883, for glycosylation analysis), heavy lysine (+8.0142) and heavy arginine (+6.0201). The target-decoy method[45,46] was employed to determine the false discovery rate (FDR). Linear discriminant analysis (LDA) was then performed to control the quality of peptide identifications using parameters such as XCorr, charge state and precursor mass accuracy,[47] which is also similar to the previous report.[48] Peptides fewer than seven amino acid residues in length were considered unreliable and deleted. Peptide spectral matches were filtered to a <1% FDR. For protein analysis, the peptide-level FDR was calculated based on all identified peptides. For glycoprotein analysis, the dataset was restricted to glycopeptides when determining FDRs for glycopeptide identification.[49,50] Furthermore, an additional protein-level filter was applied in each dataset to reduce the protein-level FDRs (<1%) for proteins and glycoproteins. Consequently the FDRs at the peptide level were much less than 1%.

Glycosylation site localization and peptide quantification

We used ModScores to assign glycosylation sites and measure the confidence of their localizations.[49,51] The ModScore software considers all possible glycosylation sites in a peptide and uses the presence of experimental fragments unique to each site to determine the actual glycosylation site and calculates a ModScore value based on the binominal probability P (ModScore = $-10 \times \log_{10}(P)$). We considered ModScore >13 ($P < 0.05$) as confidently localized. If the same peptide was quantified several times, the median heavy-to-light (H/L) value was used as the peptide abundance change. For peptides used for proteome analysis, we required that either its heavy or light isotope peak had a signal-to-noise ratio (S/N) greater than 3. If the S/N of the heavy peak was less than 3, then we required that the light peak had an S/N great than 5, and *vice versa*. Two criteria were applied for glycosylation site quantification: (1) the quantified glycopeptide must contain only one glycosylation site; (2) the site must be confidently localized with a ModScore >13.

Results and discussion

Tunicamycin treatment and glycoprotein enrichment

Tunicamycin has been widely used to model specific types of stress that affect protein folding in the ER.[52,53] However, the protein abundance changes in tunicamycin-treated cells have remained unexplored on a large scale. Our first aim was to study the proteome changes resulting from the TM treatment. Because TM is known to inhibit the formation of the *N*-acetylglucosamine-dolichol-phosphate intermediate and thus prevents protein *N*-glycosylation, we also systematically investigated *N*-glycoproteome alterations in TM-treated yeast cells. Since many membrane proteins are known to be glycosylated, 0.5% sodium deoxycholate (SDC) was added into the lysis buffer to increase membrane protein extraction. As a detergent, SDC can disrupt and dissociate many types of protein interactions, and also increase the solubility of membrane proteins. After cell lysis, protein extraction and purification, 0.5 mg of digested peptides were separated into 20 fractions using high-pH reversed phase liquid chromatography (Fig. 1). In combination with further separation under acidic conditions during on-line LC-MS/MS analysis, two-dimensional orthogonal separation can minimize peptide peak

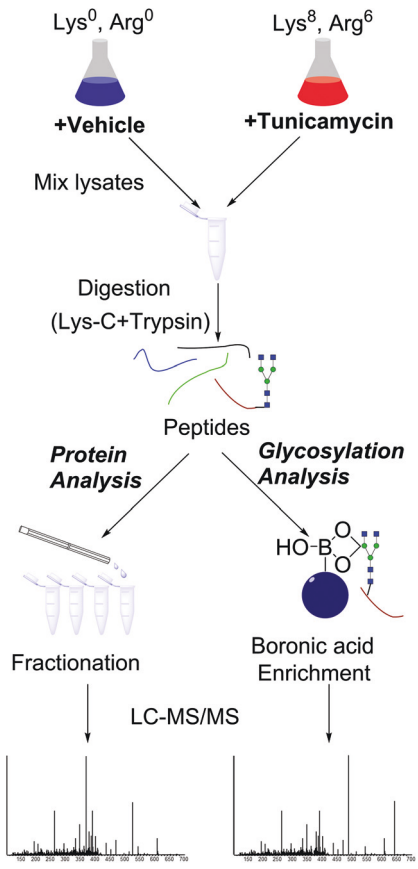

Fig. 1 Experimental procedure for the global analysis of proteins and *N*-glycoproteins in TM-treated yeast cells *vs.* untreated cells.

overlap and boost the identification of low-abundance proteins.

Two technical challenges must be overcome to globally study protein *N*-glycosylation by using MS-based proteomics techniques: the low expression levels of many glycoproteins, and the heterogeneity of glycan structures. Therefore an effective enrichment method and an efficient approach to generate a common tag on glycosylation sites for subsequent database searching are required. Based on one common features of glycoproteins, *i.e.* glycan structures bearing multiple hydroxyl groups, we globally enriched glycoproteins and/or glycopeptides through the universal boronic acid-*cis* diol recognition.[39] Boronic acid was immobilized onto magnetic beads to capture glycopeptides, and the reversible nature of the covalent interactions between boronic acid and diols made it possible to release glycopeptides (after the removal of non-specifically bound peptides) for further analysis. After enrichment, peptides were treated with PNGase F in heavy-oxygen water ($H_2{}^{18}O$) to remove *N*-glycans, which converted asparagine (Asn) to aspartic acid (Asp) containing heavy oxygen and created a mass shift of +2.9883 Da.[54,55] Heavy oxygen on Asp allows us to easily distinguish authentic *N*-glycosylation sites from those caused by deamidation occurring *in vitro* and *in vivo*. PNGase F treatment time was shortened to only 3 hours to minimize possible deamidation from non-glycosylation sites that occurs during the PNGase F cleavage process.

Examples of peptide and glycopeptide identification and quantification

In order to accurately quantify the protein expression and glycosylation changes, an Orbitrap mass spectrometer with high resolution and mass accuracy (Thermo hybrid LTQ-Orbitrap Elite MS) was used in this study. Fig. 2 shows examples of peptide and glycopeptide identifications and quantifications. Both peptides are from the protein PDI1 (YCL043C), which is a disulfide isomerase essential for the formation of disulfide bonds in secretory and cell-surface proteins, and may unscramble non-native disulfide bonds. In addition, it participates in the processing of unfolded protein-bound $Man_8GlcNAc_2$ oligosaccharides to $Man_7GlcNAc_2$, thereby promoting degradation in unfolded protein response (http://www.yeastgenome.org). This protein was determined to be up-regulated by 2.6 fold in TM-treated yeast cells, possibly as a result of TM interrupting the proper glycosylation of various proteins, and unfolded or misfolded proteins accumulating in the ER. Heavy isotope peaks of the peptide GLMNFVSIDAR are shown to be more than twice as intense as the light peaks in Fig. 2(a).

In TM-treated yeast cells, the glycosylation site N425 on this protein was down-regulated by 2.5 fold. The tandem mass spectra corresponding to the identification of the glycopeptide R@LAPTYQELADTYAN*ATSDVLIAK# (@-heavy arginine, #-heavy lysine and *-glycosylation site) is shown in Fig. 2(b);

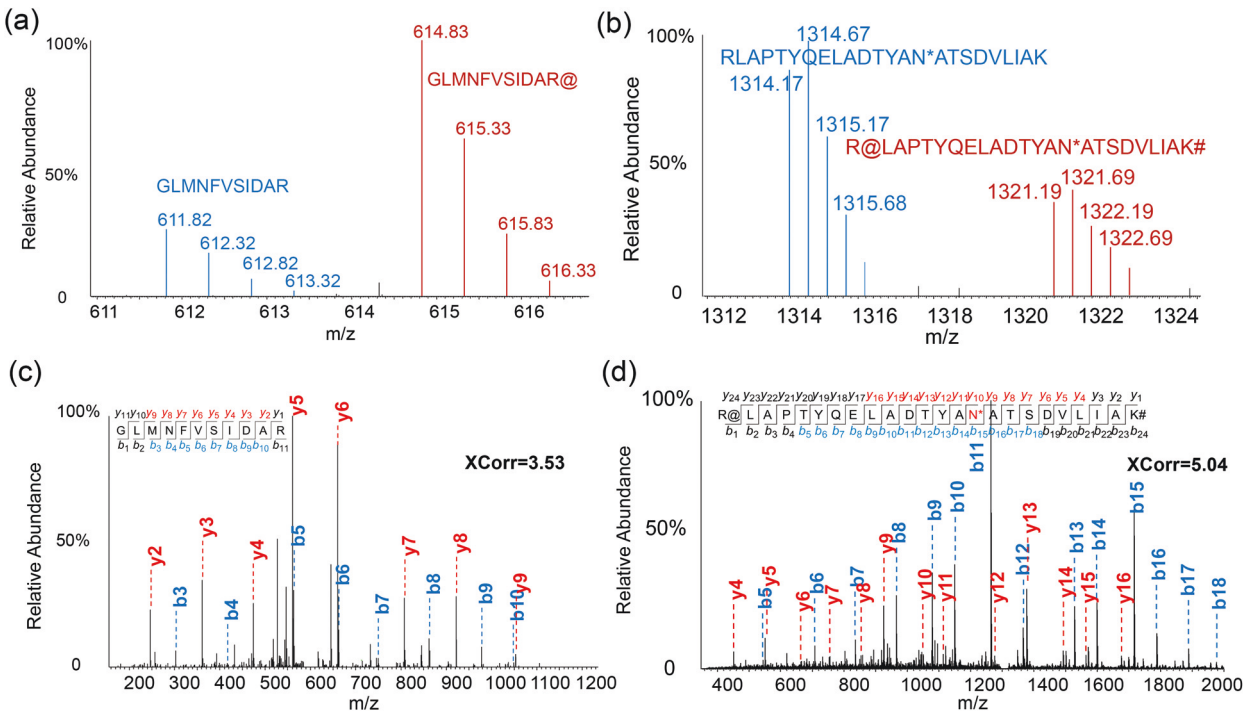

Fig. 2 Examples of full and tandem mass spectra of peptides. (a) The full and (c) tandem mass spectra of the peptide GLMNFVSIDAR and (b) the full and (d) tandem mass spectra of the glycopeptide RLAPTYQELADTYAN*ATSDVLIAK. Both peptides are from the protein PDI1. (c) and (d) demonstrated that the two peptides were confidently identified with high XCorr values. (@-heavy arginine, #-heavy lysine, *-glycosylation site).

this glycopeptide was confidently identified with an XCorr of 5.04 and a ModScore of 1000. The two ratios of peptides and glycopeptides from the same protein are excellent examples of differential protein expression and glycosylation changes resulting from the TM treatment. Several other glycosylation sites (N82, N117, N155 and N174) on this protein were also down-regulated (Table S-7†).

Global analysis of protein abundance changes

After protein samples were fractionated into 20 samples, they were measured using an online LC-MS system. With these powerful MS-based proteomics techniques, we were able to confidently quantify 4259 yeast proteins (Table S-4†), which nearly covered the entire yeast proteome.[56,57] Moreover, 95% of quantified glycoproteins were also quantified in the proteome experiments (Fig. 3(a)). Due to their low abundances, seven glycoproteins were not identified in proteome analysis without efficient glycosylation enrichment. The protein abundance change distribution is shown in Fig. 3(b) and most protein abundances did not have marked changes. Overall, 400 proteins were up-regulated while 226 proteins were down-regulated by at least 2 fold in TM-treated yeast cells. We then clustered them separately according to biological process or pathway using the Database for Annotation, Visualization, and Integrated Discovery 6.7 (DAVID 6.7).[58] Several glycan metabolism pathways, including starch and sucrose metabolism, fructose and mannose metabolism, the pentose phosphate pathway, and glycolysis-related pathways were significantly enriched among up-regulated proteins (Fig. 4(a)). This phenomenon may be due to excess glycans present in cells as a result of protein glycosylation inhibition by TM. We have quantified the majority of the proteins involved in the canonical unfolded protein response pathway,[59] including Ero1 (YML130C), an essential oxidoreductase that produces disulfide bonds in the ER, which was up-regulated by 5.2 fold. Other related proteins, including Hrd3 (YLR207W), Gcn2 (YDR283C), and Ire1 (YHR079C), had increased abundances of 1.7, 1.6, and 1.8 fold, respectively.

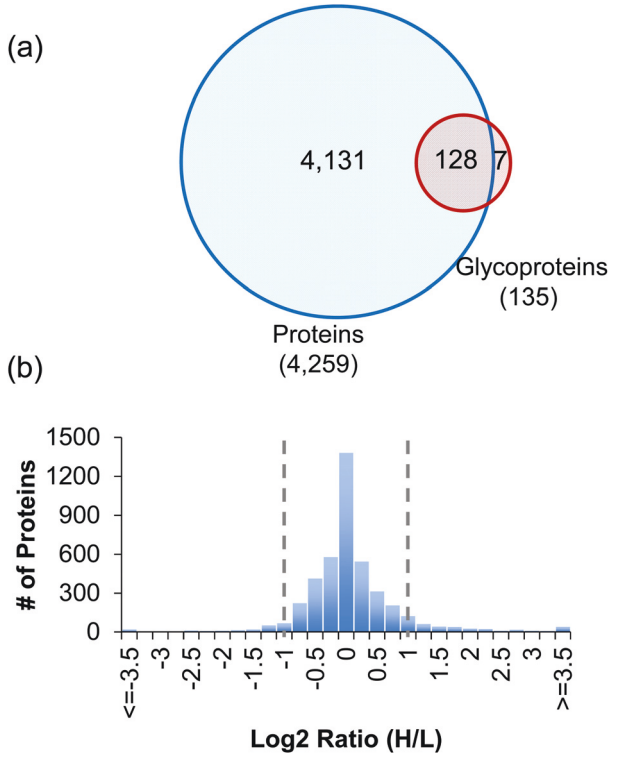

Fig. 3 Protein quantification results. (a) The overlap between proteins and glycoproteins quantified in this work. (b) The ratio distribution of quantified proteins.

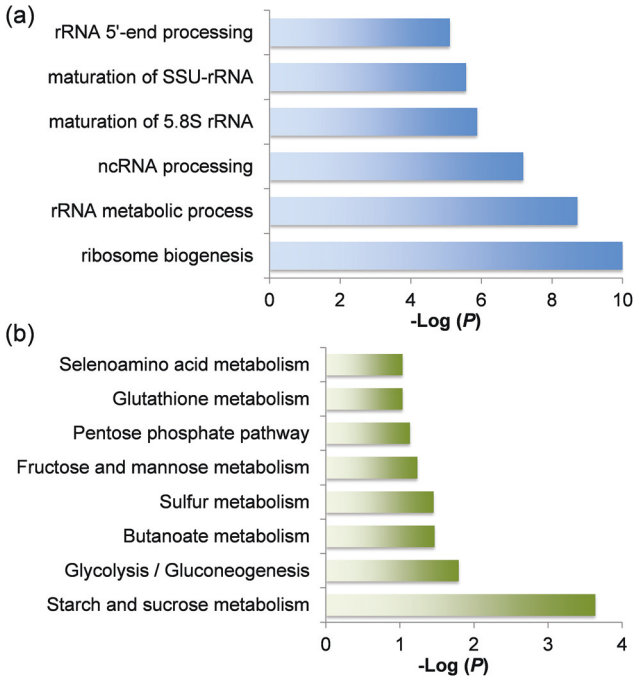

Fig. 4 Clustering of up- and down-regulated proteins in tunicamycin-treated cells. (a) Enriched pathways for up-regulated proteins. (b) Enriched biological processes among down-regulated proteins.

For down-regulated proteins, ribosome and RNA processing-related biological processes were notably enriched, which meant that protein translation was reduced. This correlates very well with previous studies in the literature.[60,61] For example, Steffen *et al.* found that ribosomal deficiency protects yeast cells against ER stress, which was a result of many secretory proteins getting trapped in the ER due to the inhibition of their glycosylation. The treatment of the ribosomal protein gene deletion strains with TM showed significant ER stress resistance.[60] In addition, protein transportation between the Golgi and plasma membrane was also attenuated. Cell wall integrity and stress response component 4 (Wsc4) is a protein that participates in protein transportation to the membrane, and cell wall biogenesis and degradation, and its expression was reduced to 6.6% as a result of a drug treatment. The dramatic down-regulation of this protein suggests that cell wall formation may be impacted in the TM-treated cells because

protein *N*-glycosylation regulates protein folding and trafficking and here it was inhibited by TM. Therefore, cell wall proteins could not be transported to the cell wall.

Site-specific glycoprotein identification

The common tag generated by PNGase F deglycosylation in heavy-oxygen water ($H_2{}^{18}O$) allowed the global and site-specific identification of protein *N*-glycosylation. As shown in Fig. 2(b), fragments in the tandem mass spectrum enabled us to confidently localize protein glycosylation sites. A total of 448 glycosylation sites were identified in the current experiment (Table S-5†). Here we assessed the confidence of site localizations with the calculation of ModScore values, which take all possible glycosylation sites in a peptide into account and uses the existing experimental fragment ions unique to each site to determine the actual glycosylation site.[39,42,49] For instance, two possible glycosylation sites located next to each other without adequate fragment ions to distinguish them will result in a low Modscore. A ModScore greater than 13 represents a *P* value less than 0.05, which we considered to be well-localized. Fig. 5(a) shows that the majority of the glycosylation site identified in this experiment are well-localized, and 68.5% of identified sites even have a ModScore larger than 19 (corresponding to a *P* value less than 0.01).

Many proteins carried multiple *N*-glycosylation sites (Fig. 5(b)) and more than 30 proteins contained at least five glycosylation sites. For example, a total of 15 glycosylation sites were identified from the protein Rax2 (YLR084C). Rax2 is required for the maintenance of the bipolar budding pattern, and is involved in selecting bud sites.[62] It was reported that Rax2 is a glycosylated type I membrane protein, with its long N-terminal domain in the extracellular space.[63] In TM-treated yeast cells, Rax2 was down-regulated by 2.07 fold while its four singly glycosylated peptides were down-regulated with ratios of 0.45, 0.46, 0.51, and 0.51, respectively.

We further investigated the correlation between the number of identified glycosylation sites and the glycoprotein length (Fig. 5(c)). It seems plausible that longer proteins could carry more glycosylation sites which would allow a greater number of glycosylation sites to be identified. When we plotted the number of glycosylation sites as a function of the protein length, there was no significant correlation between the two.

Next we considered whether protein and glycoprotein identifications in this work were biased for highly abundant proteins. Based on the number of copies (abundances) of yeast proteins reported in the literature,[64] we plotted the abundance distribution of proteins and glycoproteins identified here with the protein abundance distribution from the literature in Fig. 5(d). The *x*-axis represents the number of protein molecules per cell, and the *y*-axis shows the percentage of proteins. Despite all three protein datasets having similar distributions over various amounts of protein molecules, we quantified a considerable amount of proteins and glycoproteins that were not quantified by the tandem affinity purification (TAP)

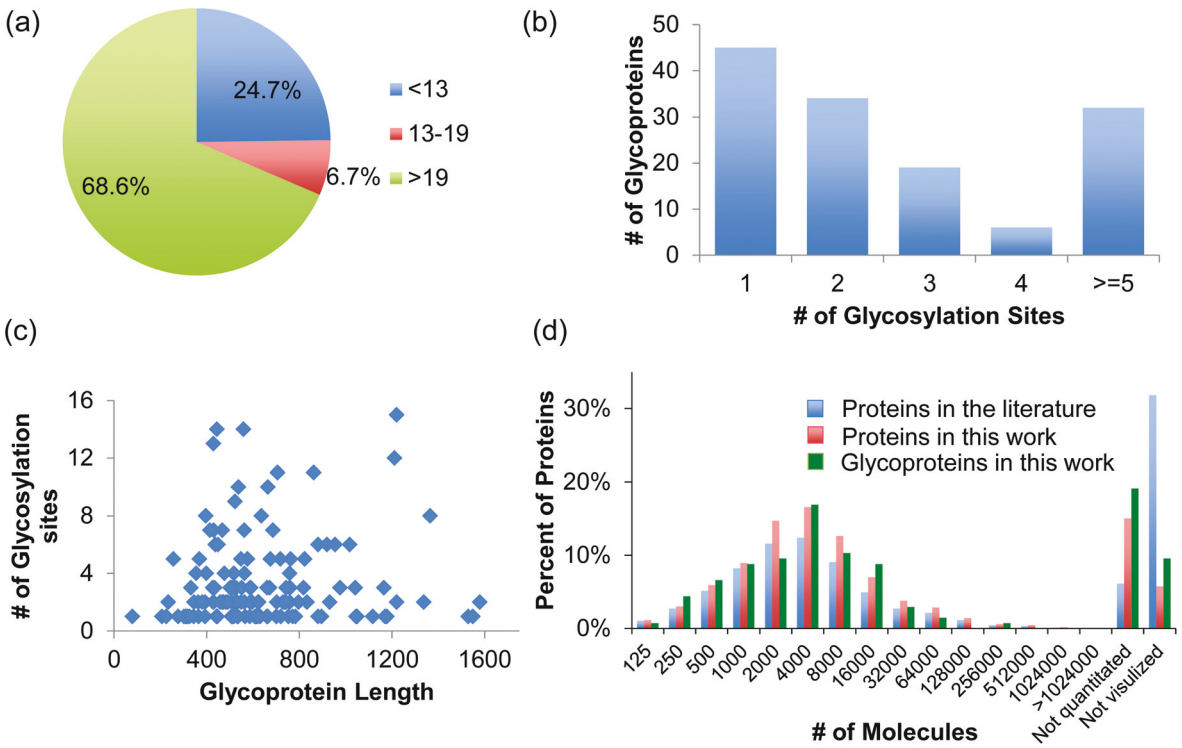

Fig. 5 The results of site-specific *N*-glycosylation identification. (a) The ModScore distribution for the identified glycosylation sites. (b) The number of glycosylation sites identified in glycoproteins. (c) The correlation between the number of glycosylation sites and the length of glycoproteins. (d) The abundance distribution of proteins and glycoproteins in the literature[64] and quantified in this work.

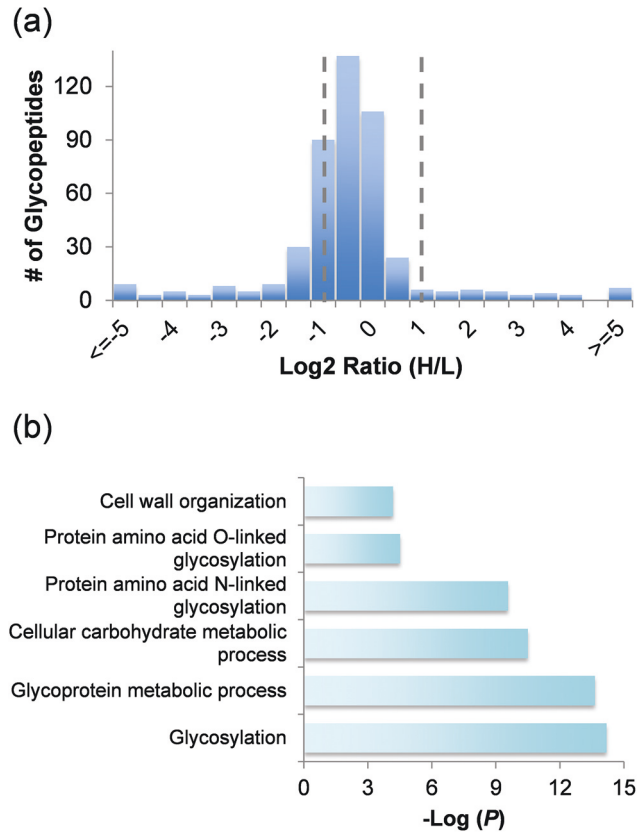

Fig. 6 The ratio distribution of glycopeptides and glycoprotein clustering. (a) Ratio distribution of the quantified glycopeptides. (b) Clustering of the down-regulated glycoproteins according to biological processes.

coupled to immune-detection method in the literature.[64] This means that modern MS methods are very sensitive and can detect proteins with very low abundances. In addition, the median length of glycoproteins identified in this experiment is 581 amino acid residues, while the yeast whole proteome (http://www.yeastgenome.org/) has a median of 359 amino acid residues. This suggested that glycoproteins are generally longer than other proteins, although the number of *N*-glycosylation sites on each protein is not always relevant to the protein length.

Quantification of glycopeptides and singly-glycosylated peptides

In this work, a total of 465 unique glycopeptides were quantified, among which more than one third (162 glycopeptides) were down-regulated by more than 2 fold, while only 40 glycopeptides were up-regulated (Table S-6†). These results are agreeable with the known glycosylation inhibition effects of TM. The distribution of glycopeptide abundances is shown in Fig. 6(a). Glycopeptides are not expected to be up-regulated as a result of tunicamycin treatment, however this could occur because some *N*-acetylglucosamine-dolichol-phosphate intermediates still exist in cells for a short period after treatment, or if the corresponding parent proteins are up-regulated. For instance, the glycopeptide R.TPLVAWGAGLNK#PVHNPFPVSDN*YTENWELSSIK#.R has an up-regulation ratio of 2.01, while the corresponding protein YKL165C were up-regulated 3.47 fold. The regulation ratio for this peptide is determined to be 0.58 after calibration. Meanwhile, peptide K.SPVETVSDSLQFSFNGN*QTK (2.34 fold) from protein YDR055W (4.65 fold) has a ratio of 0.50 after calibration. Here we only treated cells for three hours, but more glycopeptides are anticipated to be down-regulated if cells are treated for a longer time.

Glycoproteins containing down-regulated glycopeptides were clustered according to biological processes using DAVID 6.7 (Fig. 6(b)). The glycosylation, glycoprotein metabolic processes, carbohydrate processes, and cell wall organization were highly enriched. Compared to proteome analysis results, these more directly reflect the primary impact of inhibiting protein *N*-glycosylation by TM in yeast cells. Interestingly, several proteins containing down-regulated *N*-glycopeptides were related to protein *O*-glycosylation. A total of five glycoproteins in the current results were involved in this process, among which three were also involved in protein *N*-glycosylation. The other two glycoproteins, dolichyl-phosphate-mannose-protein mannosyltransferase 2 (PMT2, YAL023C) and PMT5 (YDL093W) are glycosyltransferases that participate in protein *O*-glycosylation (especially O-linked mannosylation). The current results suggest that TM treatment could also interfere with protein *O*-glycosylation by suppressing the *N*-glycosylation of important *O*-glycosylation transferases.

Table 1 Down-regulated glycosylation sites involved in the high-mannose type *N*-glycan biosynthesis pathway ($P = 1.2 \times 10^{-4}$)

Reference	Peptide	Site	Mod Score	PPM	XCorr	H/L ratio	Annotation
YJR131W	K.YLAYLTGN*R.T	224	1000	1.02	2.16	0.01	Endoplasmic reticulum mannosyl-oligosaccharide 1,2-alpha-mannosidase (MNS1)
	R.MLGGLLSAYHLSDVLEVGN*K.T	155	1000	0.16	3.33	0.44	
YER001W	K.MFPFINN*FTTETFHEMVPK.I	254	17.0	−1.21	2.52	0.04	Alpha-1,3-mannosyltransferase (MNN1)
	K.TLN*ATFPNYDPDNFK.K	225	65.4	1.75	4.74	0.05	
	R.SPDFKPVENNYDN*STNVPQEIWFLDVSNTIHPK.W	383	38.3	−3.16	5.77	0.17	
YJL186W	K.FTDTLSGKLN*FSIPQR.E	136	1000	−0.77	3.51	0.41	Alpha-1,2-mannosyltransferase (MNN5)
YPL053C	K.SYGGN*ETTLGFMVPSYINHR.G	98	145.0	−0.2	3.76	0.48	Mannosyltransferase (KTR6)

*Glycosylation site.

Finally, we extracted all the singly-glycosylated glycopeptides with a ModScore larger than 13, and performed quantification at the glycosylation site level. The ratio distribution (Fig. S-1(a)†) of quantified glycosylation sites is largely similar to that of quantified glycopeptides. A total of 253 sites were quantified, among which 81 were down-regulated and 18 were up-regulated (Table S-7†). Clustering analysis also revealed that glycosylation was impacted (Fig. S-1(b)†). The high-mannose type *N*-glycan biosynthesis pathway was found to be down-regulated with a *P* value of 1.24×10^{-4}; all sites quantified in this pathway were well-localized (Table 1). Powerful MS-based proteomics methods allowed us to systematically and site-specifically quantify protein *N*-glycosylation changes in TM-treated cells, offering valuable insight into tunicamycin–cell interactions.

Conclusion

Tunicamycin has been widely used to manipulate protein *N*-glycosylation, but the global analysis of protein expression and *N*-glycosylation changes as a result of tunicamycin treatment remains unexplored. Using Baker's yeast as a model system, we systematically investigated the protein abundance and *N*-glycosylation changes by powerful MS-based proteomics techniques. Through combination with SILAC, we have quantified 4259 proteins in tunicamycin-treated yeast cells. The majority of protein abundances changed marginally, but >5% of quantified proteins were down-regulated by >2 fold, among which proteins related to several glycan metabolism and glycolysis-related pathways were highly enriched. In addition, several proteins in the canonical unfolded protein response pathway were up-regulated because the inhibition of *N*-glycosylation dramatically impacts the proper folding and subsequent trafficking of some proteins.

We comprehensively quantified protein *N*-glycosylation changes in yeast cells induced by tunicamycin by combining boronic acid-based glycopeptide enrichment, enzymatic deglycosylation in heavy-oxygen water, and MS-based proteomics. More than one third (168) of 465 quantified unique glycopeptides were down-regulated in yeast cells with three-hour treatment. Among down-regulated glycoproteins, those related to glycosylation, glycoprotein metabolic processes, carbohydrate processes, and cell wall organization were highly enriched. The high-mannose type *N*-glycan biosynthesis pathway was also found to be down-regulated. For the first time, we systematically and quantitatively investigated protein expression and *N*-glycosylation changes in tunicamycin-treated yeast cells. These results will provide a better understanding of how cells interact with tunicamycin and how *N*-glycosylation is affected as a result.

Acknowledgements

This work is supported by the National Science Foundation (CAREER Award, CHE-1454501).

References

1 A. Herscovics and P. Orlean, *FASEB J.*, 1993, **7**, 540–550.
2 S. Defaus, P. Gupta, D. Andreu and R. Gutierrez-Gallego, *Analyst*, 2014, **139**, 2944–2967.
3 T. Kurcon, Z. Y. Liu, A. V. Paradkar, C. A. Vaiana, S. Koppolu, P. Agrawal and L. K. Mahal, *Proc. Natl. Acad. Sci. U. S. A.*, 2015, **112**, 7327–7332.
4 K. L. Hsu, K. T. Pilobello and L. K. Mahal, *Nat. Chem. Biol.*, 2006, **2**, 153–157.
5 H. J. An, S. R. Kronewitter, M. L. A. de Leoz and C. B. Lebrilla, *Curr. Opin. Chem. Biol.*, 2009, **13**, 601–607.
6 S. A. Brooks, T. M. Carter, L. Royle, D. J. Harvey, S. A. Fry, C. Kinch, R. A. Dwek and P. M. Rudd, *Anti-Cancer Agents Med. Chem.*, 2008, **8**, 2–21.
7 H. H. Freeze, J. X. Chong, M. J. Bamshad and B. G. Ng, *Am. J. Hum. Genet.*, 2014, **94**, 161–175.
8 M. M. Fuster and J. D. Esko, *Nat. Rev. Cancer*, 2005, **5**, 526–542.
9 T. Z. Ju, V. I. Otto and R. D. Cummings, *Angew. Chem., Int. Ed.*, 2011, **50**, 1770–1791.
10 L. R. Ruhaak, S. Miyamoto and C. B. Lebrilla, *Mol. Cell. Proteomics*, 2013, **12**, 846–855.
11 E. P. Go, A. Herschhorn, C. Gu, L. Castillo-Menendez, S. J. Zhang, Y. D. Mao, H. Y. Chen, H. T. Ding, J. K. Wakefield, D. Hua, H. X. Liao, J. C. Kappes, J. Sodroski and H. Desaire, *J. Virol.*, 2015, **89**, 8245–8257.
12 P. Burda and M. Aebi, *Biochim. Biophys. Acta, Gen. Subj.*, 1999, **1426**, 239–257.
13 A. Varki, R. D. Cummings, J. D. Esko, H. H. Freeze, P. Stanley, C. R. Bertozzi, G. W. Hart and M. E. Etzler, *Essentials of Glycobiology*, Cold Spring Harbor Laboratory Press, Cold Spring Harbor, New York, 2nd edn, 2008.
14 M. A. Kukuruzinska, M. L. E. Bergh and B. J. Jackson, *Annu. Rev. Biochem.*, 1987, **56**, 915–944.
15 S. Wildt and T. U. Gerngross, *Nat. Rev. Microbiol.*, 2005, **3**, 119–128.
16 T. R. Gemmill and R. B. Trimble, *Biochim. Biophys. Acta, Gen. Subj.*, 1999, **1426**, 227–237.
17 L. Lehle, S. Strahl and W. Tanner, *Angew. Chem., Int. Ed.*, 2006, **45**, 6802–6818.
18 A. Takatsuk and G. Tamura, *J. Antibiot.*, 1971, **24**, 224–231.
19 L. Lehle and W. Tanner, *FEBS Lett.*, 1976, **71**, 167–170.
20 A. F. M. Altelaar, J. Munoz and A. J. R. Heck, *Nat. Rev. Genet.*, 2013, **14**, 35–48.
21 L. N. Wang, L. Yang, L. Pan, N. R. Kadasala, L. Xue, R. J. Schuster, L. L. Parker, A. Wei and W. A. Tao, *J. Am. Chem. Soc.*, 2015, **137**, 12772–12775.
22 S. B. Ficarro, M. L. McCleland, P. T. Stukenberg, D. J. Burke, M. M. Ross, J. Shabanowitz, D. F. Hunt and F. M. White, *Nat. Biotechnol.*, 2002, **20**, 301–305.
23 D. F. Zielinska, F. Gnad, J. R. Wisniewski and M. Mann, *Cell*, 2010, **141**, 897–907.
24 S. Pankow, C. Bamberger, D. Calzolari, S. Martinez-Bartolome, M. Lavallee-Adam, W. E. Balch and J. R. Yates, *Nature*, 2015, **528**, 510–516.

25 N. Leymarie, E. A. Berg, M. E. McComb, P. B. O'Connor, J. Grogan, F. G. Oppenheim and C. E. Costello, *Anal. Chem.*, 2002, **74**, 4124–4132.
26 R. R. O. Loo and J. A. Loo, *Anal. Chem.*, 2007, **79**, 1115–1125.
27 T. Bing, D. Shangguan and Y. S. Wang, *Mol. Cell. Proteomics*, 2015, **14**, 2692–2700.
28 M. Wuhrer, M. I. Catalina, A. M. Deelder and C. H. Hokke, *J. Chromatogr., B: Biomed. Appl.*, 2007, **849**, 115–128.
29 J. C. Tran, L. Zamdborg, D. R. Ahlf, J. E. Lee, A. D. Catherman, K. R. Durbin, J. D. Tipton, A. Vellaichamy, J. F. Kellie, M. X. Li, C. Wu, S. M. M. Sweet, B. P. Early, N. Siuti, R. D. LeDuc, P. D. Compton, P. M. Thomas and N. L. Kelleher, *Nature*, 2011, **480**, 254–U141.
30 L. L. Sun, A. S. Hebert, X. J. Yan, Y. M. Zhao, M. S. Westphall, M. J. P. Rush, G. J. Zhu, M. M. Champion, J. J. Coon and N. J. Dovichi, *Angew. Chem., Int. Ed.*, 2014, **53**, 13931–13933.
31 D. C. Frost, T. Greer and L. J. Li, *Anal. Chem.*, 2015, **87**, 1646–1654.
32 B. F. Chen, Y. Peng, S. G. Valeja, L. C. Xiu, A. J. Alpert and Y. Ge, *Anal. Chem.*, 2016, **88**, 1885–1891.
33 J. G. Abelin, P. D. Trantham, S. A. Penny, A. M. Patterson, S. T. Ward, W. H. Hildebrand, M. Cobbold, D. L. Bai, J. Shabanowitz and D. F. Hunt, *Nat. Protoc.*, 2015, **10**, 1308–1318.
34 C. X. Yang, X. F. Zhong and L. J. Li, *Electrophoresis*, 2014, **35**, 3418–3429.
35 M. D. Hirschey and Y. M. Zhao, *Mol. Cell. Proteomics*, 2015, **14**, 2308–2315.
36 A. L. Richards, A. E. Merrill and J. J. Coon, *Curr. Opin. Chem. Biol.*, 2015, **24**, 11–17.
37 W. X. Chen, J. M. Smeekens and R. H. Wu, *Chem. Sci.*, 2016, **7**, 1393–1400.
38 S. S. Sun, P. Shah, S. T. Eshghi, W. M. Yang, N. Trikannad, S. Yang, L. J. Chen, P. Aiyetan, N. Hoti, Z. Zhang, D. W. Chan and H. Zhang, *Nat. Biotechnol.*, 2016, **34**, 84–88.
39 W. X. Chen, J. M. Smeekens and R. H. Wu, *Mol. Cell. Proteomics*, 2014, **13**, 1563–1572.
40 H. P. Xiao, G. X. Tang and R. H. Wu, *Anal. Chem.*, 2016, **88**, 3324–3332.
41 J. M. Smeekens, W. X. Chen and R. H. Wu, *J. Am. Soc. Mass Spectrom.*, 2015, **26**, 604–614.
42 W. X. Chen, J. M. Smeekens and R. H. Wu, *J. Proteome Res.*, 2014, **13**, 1466–1473.
43 H. P. Xiao, W. X. Chen, G. X. Tang, J. M. Smeekens and R. H. Wu, *J. Proteome Res.*, 2015, **14**, 1600–1611.
44 J. K. Eng, A. L. McCormack and J. R. Yates, *J. Am. Soc. Mass Spectrom.*, 1994, **5**, 976–989.
45 J. E. Elias and S. P. Gygi, *Nat. Methods*, 2007, **4**, 207–214.
46 J. M. Peng, J. E. Elias, C. C. Thoreen, L. J. Licklider and S. P. Gygi, *J. Proteome Res.*, 2003, **2**, 43–50.
47 E. L. Huttlin, M. P. Jedrychowski, J. E. Elias, T. Goswami, R. Rad, S. A. Beausolei, J. Villen, W. Haas, M. E. Sowa and S. P. Gygi, *Cell*, 2010, **143**, 1174–1189.
48 L. Kall, J. D. Canterbury, J. Weston, W. S. Noble and M. J. MacCoss, *Nat. Methods*, 2007, **4**, 923–925.
49 S. A. Beausoleil, J. Villen, S. A. Gerber, J. Rush and S. P. Gygi, *Nat. Biotechnol.*, 2006, **24**, 1285–1292.
50 W. X. Chen, J. M. Smeekens and R. H. Wu, *Chem. Sci.*, 2015, **6**, 4681–4689.
51 W. Kim, E. J. Bennett, E. L. Huttlin, A. Guo, J. Li, A. Possemato, M. E. Sowa, R. Rad, J. Rush, M. J. Comb, J. W. Harper and S. P. Gygi, *Mol. Cell*, 2011, **44**, 325–340.
52 C. Hammond, I. Braakman and A. Helenius, *Proc. Natl. Acad. Sci. U. S. A.*, 1994, **91**, 913–917.
53 S. S. Sun and H. Zhang, *Anal. Chem.*, 2015, **87**, 11948–11951.
54 H. Kaji, H. Saito, Y. Yamauchi, T. Shinkawa, M. Taoka, J. Hirabayashi, K. Kasai, N. Takahashi and T. Isobe, *Nat. Biotechnol.*, 2003, **21**, 667–672.
55 B. Wollscheid, D. Bausch-Fluck, C. Henderson, R. O'Brien, M. Bibel, R. Schiess, R. Aebersold and J. D. Watts, *Nat. Biotechnol.*, 2009, **27**, 378–386.
56 L. M. F. de Godoy, J. V. Olsen, J. Cox, M. L. Nielsen, N. C. Hubner, F. Frohlich, T. C. Walther and M. Mann, *Nature*, 2008, **455**, 1251–1254.
57 R. H. Wu, N. Dephoure, W. Haas, E. L. Huttlin, B. Zhai, M. E. Sowa and S. P. Gygi, *Mol. Cell. Proteomics*, 2011, **10**, DOI: 10.1074/mcp.M1111.009654.
58 D. W. Huang, B. T. Sherman and R. A. Lempicki, *Nucleic Acids Res.*, 2009, **37**, 1–13.
59 G. S. Hotamisligil, *Nat. Med.*, 2010, **16**, 396–399.
60 K. K. Steffen, M. A. McCormick, K. M. Pham, V. L. MacKay, J. R. Delaney, C. J. Murakami, M. Kaeberlein and B. K. Kennedy, *Genetics*, 2012, **191**, 107–118.
61 C. Horigome, T. Okada, K. Matsuki and K. Mizuta, *Biosci. Biotechnol., Biochem.*, 2008, **72**, 1080–1086.
62 T. Chen, T. Hiroko, A. Chaudhuri, F. Inose, M. Lord, S. Tanaka, J. Chant and A. Fujita, *Science*, 2000, **290**, 1975–1978.
63 P. J. Kang, E. Angerman, K. Nakashima, J. R. Pringle and H. O. Park, *Mol. Biol. Cell*, 2004, **15**, 5145–5157.
64 S. Ghaemmaghami, W. Huh, K. Bower, R. W. Howson, A. Belle, N. Dephoure, E. K. O'Shea and J. S. Weissman, *Nature*, 2003, **425**, 737–741.